

1 Genetic Variation Regulates Opioid-Induced Respiratory Depression in Mice

2

3

4

5

⁶ Jason A. Bubier¹, Hao He¹, Vivek M. Philip¹, Tyler Roy, Christian Monroy Hernandez, Kevin D.

7 Donohue^{2,3} Bruce F. O'Hara^{2,4}, Elissa J. Chesler^{1*}

8 ¹The Jackson Laboratory, Bar Harbor ME 04605;

9 ²Signal Solutions, LLC, Lexington, KY;

10 ³Electrical and Computer Engineering Department, University of Kentucky, Lexington, KY;

11 ⁴Department of Biology, University of Kentucky, Lexington KY

12 *Corresponding author elissa.chesler@jax.org

13 RUNNING TITLE:

14 KEY WORDS:

15

16 Specs-Scientific Reports (4.122, preprint ok)

17 Title (20 Words)

18 Abstract (200 words)

19 Introduction (4500 words with Results and Discussion) (3473 as of 4/28)

20 Results (with subheadings)

21 Discussion (without subheadings)

22 Methods (Methods section to 1,500 words) (1050 words)

23 Figure legends are limited to 350 words; no more than 8 display items

24 **Abstract**

25 In the U.S., opioid prescription for treatment of pain nearly quadrupled from 1999 to 2014, leading to an
26 epidemic in addiction and overdose deaths. The most common cause of opioid overdose and death is
27 opioid-induced respiratory depression (OIRD), a life-threatening depression in respiratory rate thought to
28 be caused by stimulation of opioid receptors in the inspiratory-generating regions of the brain. Studies in
29 mice have revealed that variation in opiate lethality is associated with strain differences, suggesting that
30 sensitivity to OIRD is genetically determined. We first tested the hypothesis that genetic variation in
31 inbred strains of mice influences the innate variability in opioid-induced responses in respiratory
32 depression, recovery time and survival time. Using the founders of the advanced, high-diversity mouse
33 populations, the Collaborative Cross (CC) and Diversity Outbred (DO), we found substantial sex and
34 genetic effects on respiratory sensitivity and opiate lethality. To define genetic modifiers of OIRD, we
35 then used the high precision DO population treated with morphine to map and identify quantitative trait
36 loci (QTL) for respiratory depression, recovery time and survival time. Trait mapping and integrative
37 functional genomic analysis in GeneWeaver has allowed us to implicate *Galnt11*, an N-
38 acetylgalactosaminyltransferase, as a candidate gene that regulates OIRD.

39

40

41

42 **Introduction**

43 One in every four individuals treated for pain with prescription opioids such as morphine
44 becomes addicted and progresses to illicit synthetic opioid use¹. The non-uniform composition, dosing
45 and administration of more potent synthetic street opioids including fentanyl frequently leads to overdose.
46 Remedial measures such as treatment with naloxone, a competitive antagonist of the opioid receptor mu 1
47 (OPRM1), the principal target of opioids, are often unsuccessful due to the higher potency of synthetic
48 opioids²⁻⁴. Therefore, novel approaches toward understanding opioid addiction, overdose and remediation
49 are essential.

50 The most frequent cause of overdose death due to opioids is opioid-induced respiratory
51 depression (OIRD). Opioids such as morphine depress the hypoxic ventilatory response in the brainstem
52 by affecting the chemosensitive cells that respond to changes in the partial pressures of carbon dioxide
53 and oxygen in the blood⁵. Understanding the underlying molecular mechanisms that control the
54 respiratory responses to opioids may provide insight into alternative therapies for opioid overdose by
55 treating the respiratory depression directly, independent of, or together with opioid receptor antagonism.
56 Variable responses in OIRD have been well documented in both humans and mice⁶, and likely occur
57 through diversity in the molecular pathways within the ventilatory processing centers of the brainstem.
58 Our goal is to utilize this genetic diversity to define genetic modifiers of OIRD in mice.

59 Genetic diversity in laboratory mice is a powerful tool for dissecting the genetic and molecular
60 components of complex traits such as the response to opioids. In mice, genetic variation has been
61 identified in the opioid receptors⁷⁻¹¹, in genes and pathways associated with the anti-nociceptive effects of
62 morphine¹²⁻¹⁷ and morphine withdrawal¹⁸, and in other behavioral responses to opioids^{16,19,20}. Other
63 studies have characterized the median lethal dose (LD₅₀) of morphine across mouse strains²¹⁻²³. One study
64 found that a strain harboring an OPRM1 hypomorph (CXB7), in which OPRM1 gene function is reduced,
65 have a much higher LD₅₀ for morphine than strains with intact mu-opioid^{8,24}, confirming the importance
66 of OPRM1 in opioid-induced lethality and revealing strain diversity in the mu-opioid receptor locus.

67 Together, these studies show that variation in response to opioids is associated with differences in strain,
68 indicating that responses to opioids are genetically influenced phenotypes. However, these studies were
69 generally conducted on only a few strains of male mice with survival as the only endpoint, and thus did
70 not characterize known sex differences in opioid sensitivity²⁵ and were not designed to define the genetic
71 loci or the underlying biological mechanisms responsible for the strain variation in complex opioid
72 responses, such as respiratory depression.

73 Respiratory phenotyping in mice generally includes measures of ventilation mechanics such as
74 respiratory frequency and tidal volume using conventional plethysmography. However, plethysmography
75 is labor intensive and the duration over which the mouse can be monitored is limited because the animal
76 is confined and its movements are restricted. Further, monitoring the rapid response to drugs by
77 plethysmography is invasive because it requires the surgical implantation of a cannula, catheter or other
78 port into the mouse in order to administer the compounds. Here, we have taken the novel approach using
79 signals obtained from a piezo electric sleep monitoring system²⁶ to measure respiratory phenotypes. This
80 system offers a non-invasive, high-throughput technology to study respiratory depression in response to
81 opioids in mice in a home-cage setting. The piezo technology was adapted to estimate average respiratory
82 rates over specified time intervals for characterizing patterns associated with respiratory depression. This
83 allows for the determination of respiratory depression and time to recovery or cessation of respiration.
84 This system was previously validated and used by us in genetic studies of sleep in the Collaborative Cross
85 (CC)^{27,28}, BXD¹⁸, and other mouse populations²⁹.

86 In this study, we investigated the effect of genetic variation on OIRD and lethality in the founders
87 of the advanced, high-diversity mouse populations, specifically the CC and Diversity Outbred (DO)
88 populations. After determining that the quantitative respiratory phenotypes were heritable and that genetic
89 mapping was therefore feasible, we mapped key respiratory traits using a population of 300 DO mice of
90 both sexes and our advanced piezo electric sleep monitoring system²⁶. This enabled us to reveal a

91 previously undiscovered potential mechanism of variability in OIRD, which was further evaluated
92 through analysis of sequence variation, gene expression and conservation of protein domains.

93

94

95 **Results**

96 **Development of a high-throughput method for measuring respiratory depression in response to**
97 **opioids.**

98 The PiezoSleep system was adapted for use as an in depth, high-throughput, continuous monitoring
99 approach for key respiratory responses to morphine. The piezoelectric transducer in the cage floor
100 produces voltage in direct proportion to the pressure applied to the cage floor. The pressure signal is
101 amplified, filtered, and digitized for processing to extract signal features related to irregular wake-like
102 activity and regular sleep-like motions primarily resulting from respiration (thorax pressure directly on
103 the cage floor or pressure variations being transferred through the legs). Although the original PiezoSleep
104 system only provides respiratory estimates during sleep, the algorithm was adapted to find periods of low
105 activity and estimate respiratory rates when breathing signals were detected. These were averaged over
106 larger intervals to provide an average respiration rate every 12 minutes to obtain a baseline rate (24 hours
107 pretreatment) that could be compared to post-treatment responses. This enabled a quantitative evaluation
108 of respiratory depression, survival time and recovery time (Fig. 1).

109 **Respiratory depression, recovery time and survival time are heritable traits.**

110 A bracketing approach was used to construct a dose-response curve with a minimal number of mice.
111 Eight inbred strains of mice (CC and DO founders) of both sexes were tested with an initial probe dose of
112 436 mg/kg of morphine. We found a wide range of outcomes for respiratory depression (49% to 77%),
113 recovery times (0.05 hours to 8.61 hours) and survival times that segregate largely by strain, but also by
114 sex (Fig. 2). Respiratory depression at the 436 mg/kg dose showed a significant effect of strain ($F_{\text{strain}}(7,80)$
115 = 10.7357, $p < 0.0001$), but no sex effect or sex \times strain interaction. Using time as the independent
116 variable, we fit a linear model that revealed significant effects of strain, sex and dose on both recovery
117 time ($F_{(25,152)} = 4.2774$; $p < 0.0001$) and survival time ($F_{(24,162)} = 10.1922$; $p < 0.0001$). From these
118 quantitative measurements, we calculated the strain intra-class correlation (ICC) as an estimate of
119 heritability and found that respiratory depression ICC = 0.440, recovery time ICC = 0.345 and survival

120 time ICC = 0.338. These values indicate that the traits are heritable and also amendable to genetic
121 mapping. All strain data have been deposited in the Mouse Phenome Database (RRID:SCR_003212
122 ProjectID:Bubier3).

123 **LD₅₀ determination.**

124 Published data reveal a variety of morphine LD₅₀ values for mice. In prior studies, using C57BL/6BY and
125 CXB7, the LD₅₀ values were 436 mg/kg and 977 mg/kg, respectively²⁴. Yoburn et. al have shown that the
126 LD₅₀ for different populations of outbred Swiss-Webster range from 313 mg/kg to 745 mg/kg.²³ Based
127 upon this literature, we selected a probe dose of 436 mg/kg. To generate the LD₅₀ curve using the
128 minimum number of mice, additional higher or lower doses of morphine were included based on the
129 response to the probe dose until an LD₅₀ could be estimated accurately, whereby doses on each side of the
130 50% mark were tested. Using this approach, survival curves by strain and sex were established (Fig. 3A)
131 and the LD₅₀ for each was determined (Fig. 3B). The morphine LD₅₀ ranged from 212.2 mg/kg in A/J
132 females to 882.2 mg/kg in CAST/EiJ females. There was not a consistent sex bias up or down across all
133 strains; instead, some LD₅₀ values were higher in females than males (e.g., CAST/EiJ and NOD/ShiLtJ),
134 but higher in males than females (e.g., PWK/PhJ and WSB/EiJ).

135 **Genetic mapping in DO mice.**

136 To find genetic loci that influence OIRD, QTL mapping was performed on the respiratory phenotypes
137 using the high diversity, high precision, DO mouse population. A probe dose of 486 mg/kg, chosen based
138 upon the average LD₅₀ of the eight founder strains and two sexes, was given to 300 DO mice, 150 of each
139 sex. Of the 300 DO mice entered into the study, 193 (83 females, 110 males) recovered and 107 (67
140 females, 40 males) did not recover. The quantitative metrics for respiratory response to morphine,
141 including respiratory depression, recovery time and survival time, all show a continuum of phenotypic
142 diversity (Fig. 4).³⁰

143 **Respiratory response QTL.**

144 We next mapped QTL in the DO for the three respiratory traits using R/qtl2³⁰ which implements an eight-
145 state additive haplotype model. A significant QTL was identified for respiratory depression, but no
146 genome-wide significant QTLs were detected for recovery time or survival time using these sample sizes.
147 One suggestive QTL was identified for overall morphine survival using a COXPH model as has
148 previously been used for QTL mapping³¹ (Fig. S1).

149 For the respiratory depression trait, we identified a LOD 9.2 QTL with a 1.5 LOD drop interval
150 on Chr 5:24.30- 26.25 (Fig. 5A). The 95% LOD score threshold was 7.65 for $p < 0.05$. The QTL is called
151 *Rdro1* (respiratory depression, response to opioids 1). The *Rdro1* QTL is driven by strong NOD vs.
152 WSB/EiJ allele effects (Fig. 5B). A two-state SNP association analysis identifies potential causative SNPs
153 and results in a reduction of the 1.5 LOD drop credible interval from the peak marker (24.98-26.16 MBp),
154 purple SNPs in Fig 5C. An ANOVA shows that the peak marker for the respiratory depression phenotype
155 accounts for 42.8% of heritable variation in the DO population.

156 **Identification of candidate genes.**

157 Genetic mapping studies are used to identify regions of interest containing variants that influence
158 complex traits. To identify the relevant genes involved in complex trait regulatory mechanisms, there
159 must be evidence of genetic polymorphisms segregating in the population that either influence protein
160 structure or gene expression and evidence of a biological mechanism of action connecting them to the
161 trait, such as expression in a trait-relevant tissue. We identified a 24.98-26.16 MBp credible interval
162 containing 10,782 SNPs (including insertions and deletions) across the DO mice. More specifically using
163 the SNP association mapping model, we found that 1,885 of these SNPs alleles were in the interval (Fig.
164 5B, Table S1). Of these 1,885 SNPs, eight were in coding regions of genes, 11 were in 5'UTRs, 16 were
165 in 3'UTRs, 861 were intronic, 932 were intergenic, and 107 were in non-coding transcripts (some SNPs
166 have multiple functions, Table S1). Non-coding variants typically influence phenotype through effects on
167 regulation of gene expression via SNPs in regulatory regions often located in the 5' UTR, 3' UTR,
168 introns or within intergenic regulator features. These potential regulatory SNPs are all located in

169 *Speer4a*, *Actr3b*, *Xrcc2*, *Kmt2c*, *Galnt5*, and *Prkag2*. While these SNPs remain candidates for regulation
170 of the respiratory depression phenotype, we focused on coding SNPs because their impact is more readily
171 predictable. The eight coding SNPs lie in four genes (*Galnt11*, *Kmt2c*, *Speer4a*, and *Galnt5*). None of
172 the coding SNPs are the type with the most deleterious effects, such as a stop loss, stop gain or coding
173 region insertion (frameshift). All four of these protein-coding genes are expressed in the mouse pre-
174 Bötzinger complex, a group of brainstem interneurons that control regulation of respiratory
175 rythmogenicity³², and are thus mechanistically plausible. Three of these four pre-Bötzinger complex-
176 expressed protein-coding genes contain polymorphisms that cause non-synonymous (Cn) amino acid
177 changes. Two of the three changes (serine to threonine at amino acid 702 in *Kmt2c* and asparagine to
178 aspartic acid at amino acid 29 in *Speer4a*) occurred in residues that are not conserved across species. The
179 remaining gene expressed in the pre-Bötzinger complex and containing a SNP in a conserved coding
180 region is polypeptide N-acetylgalactosaminyltransferase 11 (*Galnt11*).

181 **Galnt11 SNP analysis**

182 The *Galnt11* SNP, rs37913166 C/T, changes polar serine residue 545 to a hydrophobic leucine residue
183 (Fig. 6). This amino acid is located within a functional domain that is conserved in vertebrates (Fig. 7A),
184 suggesting that this base change regulates a key functionality. Indeed, this change places the hydrophobic
185 residue, which are generally buried internally, onto the surface of the protein. The 3D protein structure
186 analysis (Fig. 7B) indicates that the non-synonymous serine-to-leucine SNP occurs in a conserved residue
187 within the functional Ricin B lectin domain, a domain generally involved in sugar binding required for
188 glycosylation.

189 **Integrative functional genomic analysis.**

190 *GALTN11* is a member of a family of an N-acetylgalactosaminyltransferases, which function in O-linked
191 glycosylation. The non-synonymous serine-to-leucine SNP changes a conserved residue within the Ricin
192 B lectin domain of *GALNT11* and would be predicted to impede O-linked glycosylation. *GALTN11* has

193 been shown to uniquely glycosylate at least 313 glycoproteins in HEK cells³³. Using the Jaccard
194 similarity tool in the GeneWeaver³⁴ system for integrative functional genomics, we determined that of the
195 313 human glycopeptides, 287 mouse orthologs are expressed in the mouse pre-Bötzinger complex³²
196 (Table S2). Four of those genes *Hs6st2*³⁵, *Fnl*³⁶, *Lrp1*³⁵, and *Sdc4*³⁷ were identified by the Comparative
197 Toxicogenomic Database³⁸ as morphine-associated genes, and one additional pre-Bötzinger-expressed
198 glycoprotein, *Cacna2d1*, has been shown to have differential brain expression in mice following
199 morphine treatment³⁹. Therefore, variants in *Galnt11* have a plausible mechanism of action through
200 regulation of morphine-associated peptides in the pre-Bötzinger complex.

201 **Discussion**

202 In this study, we found heritable strain differences in the quantitative metrics of respiratory response to
203 morphine, including respiratory depression, recovery time and survival time, using an advanced, high-
204 throughput, behavioral phenotyping protocol. We further identified genomic loci involved in morphine-
205 induced respiratory depression using an unbiased genetic approach. Mapping these traits in the DO mice
206 and evaluation of sequence variants and protein structure, followed by integrative functional genomic
207 analysis in GeneWeaver, has allowed us to implicate *Galnt11* as a candidate gene for respiratory
208 depression in response to morphine.

209 We identified specific inbred strains of mice that were more sensitive to morphine than other
210 inbred strains of mice. The effect of sex was bidirectional in the inbred CC/DO founder strain population
211 where some males and females differed from each other in either direction depending on strain. The traits
212 of respiratory depression, recovery time and survival time were all shown to have a high degree of
213 heritability and were largely independent traits. In determining our probe dose for the outbred population,
214 we observed that the LD₅₀ for morphine differed by four-fold between these eight parental strains
215 harboring 45 million SNPs, or an equivalent genetic variation as found in the human population.
216 Interestingly, mice such as AJ that had the lowest LD₅₀ for both males and females, did not demonstrate

217 the highest degree of respiratory depression, suggesting that factors other than respiratory depression may
218 play a role in opioid overdose.

219 To date, there have been no human GWAS or linkage studies for OIRD. Several GWAS studies
220 have evaluated opioid use disorder (OUD) and/or opioid dependence, and have identified a variety of loci
221 including SNPs linked to OPRM1, KCNG2, CNIH3, LOC647946, LOC101927293, CREB1, PIK3C3,
222 and RGMA⁴⁰⁻⁴⁵. Additional human linkage studies have identified sex-specific traits⁴⁶, epigenetic
223 biomarkers⁴⁷ or copy number variations⁴⁸ for risk of OUD. Other studies have sought to separate opioid
224 use from opioid dependence, and have thus far identified SNPs associated with SDCCAG8, SLC30A9,
225 and BEND4⁴⁹. Only one study has looked at human opioid overdose risk, specifically by scoring overdose
226 status and determining the number of times that medical treatment was needed in European American
227 populations⁵⁰. In this study, SNPs near MCOLN1, PNPLA6 and DDX18 were identified as overdose risk
228 alleles. Human genes have thus been mapped to opioid use, opioid dependence and opioid overdose
229 susceptibility but human studies are not able to assess opioid-induced respiratory depression, specifically
230 the LD₅₀ of an opioid.

231 Animal studies have allowed us the opportunity to assess the LD₅₀ of a drug in a variety of
232 genetic backgrounds and then map those sources of variation. These types of controlled exposure
233 experiments cannot be conducted in humans for which exquisite control of environment is not feasible
234 and prior exposure history is unknown. Our genetic approach of QTL mapping in the DO mouse
235 population has allowed us to identify a genomic region containing no genes previously known to function
236 in opioid pharmacodynamics or pharmacokinetic processes, or implicated in OUD. The genetically
237 diverse structure of this population allows for the identification of narrow genomic intervals often with
238 very few candidate genes. This approach of using advanced mouse populations together with integrative
239 functional genomics has been useful for the prioritization of candidate genes in a variety of different
240 disciplines⁵¹⁻⁵³

241 The identification of *Galnt11* as functioning within the morphine respiratory response reveals a
242 potential new target for therapeutic development. GALNT11 is an N-acetylgalactosaminyltransferase that
243 initiates O-linked glycosylation whereby an N-acetyl-D-galactosamine residue is transferred to a serine or
244 threonine residue on the target protein. The lectin domain of GALNT11 is the portion that functions to
245 recognize partially glycosylated substrates and direct the glycosylation at nearby sites. This type of post-
246 translational modification controls many pharmacokinetic and pharmacodynamic processes as well as the
247 regulation of delta opioid receptor (OPRD1) membrane insertions as O-linked glycosylation is required
248 for proper export of OPRD1 from the ER⁵⁴. O-linked glycosylation is also required for opioid binding
249 peptides, increasing their ability to cross the blood brain barrier⁵⁵. The integrative functional analysis in
250 GeneWeaver identified *Hs6st2*³⁵, *Fn1*³⁶, *Lrp1*³⁵, and *Sdc4*³⁷ as glycosylation targets of *Galnt11*. All are
251 expressed in the pre-Bötzinger complex and are known to be responsive to morphine further supporting
252 the concept that *Galnt11* is involved in morphine-related responses. Both *Hs6st2* and *Lrp1* were identified
253 as increasing and decreasing, respectively, in responsive to both morphine and stress in C57BL/6J mice³⁵.
254 *Fn1* was upregulated six hours post morphine but downregulated four days later³⁶, and *Sdc4*, a known-
255 mu opioid receptor-dependent gene was also upregulated by morphine³⁷. The drug-regulated expression
256 of these known glycosylation targets of GALNT11 in relevant tissues further supports the functional
257 relevance of *Galnt11* to OIRD.

258 Our findings demonstrate the initial mapping of a locus involved in OIRD in mice, for which the
259 likely candidates do not act via the opioid receptor, thereby providing a potential new target for remedial
260 measures. Although it is through mouse genetic variation that we identified this gene, it should be noted
261 that this gene or its glycosylation targets need not vary in humans to be a viable target mechanism for
262 therapeutic discovery and development. Characterization of the role of *Galnt11* and its variants along
263 with other viable candidates will resolve the mechanism further, and continued mapping studies in larger
264 populations will enable detection of additional loci for various aspects of the opioid induced respiratory
265 response. These findings suggest that phenotypic and genetic variation in the laboratory mouse provides a
266 useful discovery tool for identification of previously unknown biological mechanisms of OIRD.

267

268 **Methods**

269 **Mice.**

270 Male (n=6) and female (n=6) mice from eight inbred strains including the founders that were used for the
271 DO and CC population [C57BL/6J, 129S1/SvImJ, A/J, NOD/ShiLtJ, NZO/HILtJ, /CAST/EiJ, PWK/PhJ,
272 WSB/EiJ] were tested at each dose of morphine. Male and female DO mice (n =300 including 150 of
273 each sex; J:DO, JAX stock number 009376) from generation 28 of outcrossing were used. All mice were
274 acquired from The Jackson Laboratory (JAX) and were housed in duplex polycarbonate cages and
275 maintained in a climate-controlled room under a standard 12:12 light-dark cycle (lights on at 0600 h).
276 Bedding was changed weekly and mice had free access to acidified water throughout the study. Mice
277 were provided free access to food (NIH31 5K52 chow, LabDiet/PMI Nutrition, St. Louis, MO). A Nestlet
278 and Shepherd Shack were provided in each cage for enrichment. Mice were housed in same sex groups of
279 three to five mice per cage. All procedures and protocols were approved by JAX Animal Care and Use
280 Committee and were conducted in compliance with the NIH Guidelines for the Care and Use of
281 Laboratory Animals.

282 **Morphine.**

283 Morphine sulfate pentahydrate (NIDA Drug Supply) was prepared at varying concentrations in sterile
284 saline to deliver doses (200-1200 mg/kg s.c.) in a manner not to exceed 0.2 ml/10g body weight. Starting
285 with a dose of 436 mg/kg for all strains and depending upon the result of that dose, the next dose was
286 either increased (536 mg/kg) or decreased (336 mg/kg) for the next cohort, such that doses flanking both
287 sides of the 50% survival point (LD_{50}) were tested. This was repeated with increasing and decreasing
288 doses as necessary depending upon the results of the previous dose. Not all strains received all doses but
289 each strain received at least three doses such that two flanked (one above, one below) the LD_{50} . Using this
290 approach and testing 3-4 doses per strain, the LD_{50} for the eight strains and both sexes was determined
291 and ranged from 212 mg/kg - 882 mg/kg.

292 **Piezoelectric sleep monitoring to determine respiratory depression, recovery time and survival**

293 **time.**

294 Mice were placed individually into the 7 x 7 inch piezoelectric grid and chamber system for 24 hours to
295 equilibrate to the apparatus and collect baseline activity data^{26,56}. Individual testing is necessary due to the
296 known enhanced lethality of cage mates during morphine exposure, which has been shown to affect
297 survival⁵⁷. The mice had access to food and water *ad libitum* while in the chamber. The room was
298 maintained on a 12:12-h light:dark cycle. To control for known circadian effects⁵⁸ mice were placed in the
299 chambers between 9-12 am on Day 1 and were injected with morphine 24 hours later. They remained in
300 their chambers undisturbed until 24 hours after injection. Whenever possible, complete balanced cohorts
301 of the eight strains and both sexes were run during each of nine replicates of the experiment. The data
302 acquisition computer, food and water were checked daily; otherwise, the mice remained undisturbed.
303 Breath rates were estimated from 4-second intervals in which animal activity dropped low (i.e. during
304 sleep and brief rest periods and pauses during wake), and averaged over 24-minute overlapping intervals
305 to provide an average respiratory rate every 12 minutes. The respiratory rate baseline consisted of the
306 average respiratory rate over the first 24 hours, which included both sleep and wake periods. Respiratory
307 rate was then measured in the same way after injection of opioid. These measures were then used to
308 determine thresholds for obtaining the recovery time (respiratory rate returns to baseline, see Fig. 1) or
309 survival time (animal stops moving and breathing, never returning to threshold, see Fig. 1). The 300 DO
310 mice were tested in random cohorts of 36 using the PiezoSleep system with a single 486 mg/kg dose of
311 morphine. This dose was determined as the average LD₅₀ dose across the eight strains and two sexes, 16
312 samples.

313 **Calculating respiratory depression, recovery time and survival time.**

314 To test for difference in the respiratory depression, recovery time and survival time across the strains
315 and sexes a linear model was fit, the full model was:

316
$$\text{Phenotype} = \beta_0 \text{Sex} + \beta_1 \text{Strain} + \beta_2 (\text{Sex} \times \text{Strain}) + \beta_3 \text{Dose} + \varepsilon$$

317 where Phenotype was respiratory depression, recovery time or survival time and where ϵ is random error.

318 The β -parameters were estimated by ordinary least squares, and the type III sum of squares was

319 considered ϵ in the ANOVA model. In all cases, the full model was fit and reduced by dropping non-

320 significant interactions followed by main effects.

321 **Calculating broad sense heritability (H2).**

322 As a measure of broad sense heritability in the founder strains, the ICC was determined using ICCest

323 from the ICC 2.3.4⁵⁹ package in R 4.0.0.

324 **Morphine LD₅₀ data analysis.**

325 The LD₅₀ was calculated using the drc 3.0-1 library⁶⁰ in R using the total tested and the observed dead at

326 each dose as a binary or binomial response. A logistic regression model was fit, and a goodness of fit test

327 (based upon Bates and Watts⁶¹) performed. In addition, a regression model assuming equal LD₅₀ across

328 strains was compared by chi square to an LD₅₀ assumed different across strains. An adjusted and

329 unadjusted 95% credible interval was also calculated. To graph the data a non-linear 2-parameter model

330 was fit in JMP 14.2.0 (RRID:SCR_014242) with the formula:

$$\frac{1}{\left(1 + \text{Exp} \left(-a \cdot (Dose - b) \right) \right)}$$

331

332 where a=growth rate and b=inflection point.

333 **Genotyping.**

334 Tail samples were collected at the conclusion of the experiment and all mice were genotyped using the

335 Giga-MUGA genotyping array (NeoGene). Data were deposited in the DO Database (DODB)

336 RRID:SCR_018180). Genotypes were imputed to a 69K grid to allow for equal representation across the

337 genome.

338 **QTL Mapping.**

339 Genotype probabilities were calculated according to the founder genotypes and then converted to allele
340 probabilities. We then interpolated allele probabilities into a grid of 69,000 evenly-spaced genetic
341 intervals⁶². We performed genome scans using R/qtl2 RRID:SCR_018181⁶³. Sex and date of test were
342 included as additive covariates. The model includes the random effect of kinship among the DO animals
343 computed using the LOCO method⁶⁴. The significance thresholds were determined for each trait by
344 permutation mapping⁶⁵. The confidence interval around the peak makers was determined using Bayesian
345 support intervals. To determine the percent of variation accounted for by the QTL the mice were
346 classified at the variant into one of eight states based on genotype probabilities of mice at that locus.
347 Following this, a one-way ANOVA was fit to ascertain the strain variation relative to total variation
348 towards estimating heritable variation at that locus. SNP association mapping was also performed using
349 R/qtl2 to test the association of individual SNPs alleles in the region of the locus with the phenotype.
350 Briefly, SNP data were obtained from the SANGER and MGI databases^{66,67} for the interval. Using the
351 genotype probabilities and the founder SNP genotypes to infer the SNP genotypes of the DO mice. At
352 each SNP location the eight allele state probabilities are collapsed to two state SNP probabilities are
353 collapsed to The Cox proportional hazards regression was performed by coxph function in the survival
354 (3.1-12) R package. Based on the output of the log (base e) likelihood for the null model and for the
355 alternative model (with covariates and genotype probabilities), we took the difference of both log
356 likelihoods and then divided by ln(10) to convert the results into the LOD scale. Full QTL mapping
357 scripts are available https://thejacksonlaboratory.github.io/DO_Opioid/index.html

358 **Candidate gene analysis.**

359 In order to assess the plausibility of genes in the QTL interval we identified all SNPs within the additive
360 SNP model segregating between the high and low alleles of the DO founder strains. Next we identified
361 those that were within protein coding region that were most deleterious. Differential coding sequence
362 non-synonymous amino acid substitution SNPs (Cn) that differed between the high and low allele groups

363 were identified. GeneWeaver's database (RRID:SCR_003009) was searched to identify the overlap
364 among tissue-specific expression profiles from Allen Brain Atlas as well as datasets derived from Entrez
365 GEO profiles (RRID:SCR_004584) for pre-Bötzinger neurons³² (GS 273275), diaphragm (GS273269)⁶⁸
366 and lung⁶⁹ with the QTL positional candidates,. The gene sets were overlapped using the Jaccard
367 similarity and GeneSet graph tools³⁴.

368 In order to determine if the Cn SNPs were in areas of evolutionary conservation we aligned the
369 sequence of several species. Representative sequences for each species *Drosophila* (Q8MVS5), *Xenopus*
370 (Q6DJR8), *Danio* (Q08CC3), *Rattus* (Q6P6V1), *Mus* (Q921L8), *Homo* (Q8NCW6) were acquired from
371 Uniprot (RRID:SCR_002380) and aligned. The clustalo program was used with default parameters⁷⁰. The
372 transition matrix is Gonnet, gap opening penalty of six bits, gap extension of one bit. Clustal-Omega uses
373 the HHalign algorithm and its default settings as its core alignment engine⁷¹. To determine where the
374 three-dimensional effects of the amino acid change would be we obtained the 3D crystal structure
375 (1XHB)⁷² from the Research Collaboratory for Structural Bioinformatics Protein Data Bank
376 (RRID:SCR_012820) and visualized it with Jmol (RRID:SCR_003796)⁷³.

377 **Integrative functional genomics.**

378 In order to assess the functional sufficiency of *Galnt11* as a candidate gene the literature was searched to
379 identify genome-wide studies characterizing glycosylation targets of GALTN11, one study was
380 identified³³ and these genes were added to the GeneWeaver Database (GS356053). Using the Jaccard
381 similarity tool, we overlapped the glycosylation targets with the genes expressed in the mouse pre-
382 Bötzinger complex. We next overlapped these gene with genes identified by the Comparative
383 Toxicogenomic Database (RRID:SCR_006530) as morphine-associated genes.

384

385 **Figure Legends**

386 **Figure 1.** PiezoSleep output for a mouse that recovers and a mouse that fails to recover after opioid
387 treatment. Baseline respiratory rate is first established for 24 hr. Time 0, is the time at which morphine is
388 administered. The *blue line* represents the derived respiratory rate trajectories relative to the baseline

389 (defined as the average respiratory rate over the first 24 hours (set at 100%)). Respiratory depression is
390 defined as the lowest percentage of baseline reached after morphine treatment (*purple dotted arrow*). For
391 a mouse that recovers, the *green vertical arrow* indicates recovery time when the respiratory rate returns
392 to baseline. For a mouse that does not recover, the *red vertical arrow* indicates survival time when
393 breathing stops (i.e., piezo output becomes machine noise never returning to baseline).

394

395 **Figure 2.** Strain- and sex-specific effect of morphine on respiratory sensitivity. Respiratory depression
396 (top panel), recovery time (middle panel) and survival time (bottom panel) were determined using the
397 probe dose of 436 mg/kg and the PiezoSleep system. The traits of recovery time or survival time are
398 censored such that a mouse does not appear in both graphs as each mouse displays only one of these two
399 phenotypes. Empty bars indicate that no mice fell into this category (i.e., either all recovered or none
400 recovered).

401

402 **Figure 3.** The morphine LD₅₀ by strain and sex. The morphine LD₅₀ was determined for each of the eight
403 founder strains and sex using at least six mice in each group and at least three doses of morphine, with at
404 least two doses flanking the LD₅₀. **(A)** Logistic 2-paramater survival curves separated by strain and sex
405 are shown at the top and composites of all strains separated by sex are shown at the bottom. **(B)** The LD₅₀
406 as calculated using the drc package in R and ranged from 212 mg/kg - 882 mg/kg.

407

408 **Figure 4.** Respiratory response to morphine in Diversity Outbred mice. DO mice were given 486 mg/kg
409 dose of morphine and the respiratory responses were determined by the Piezo Sleep system. The
410 distribution of respiratory responses is shown for respiratory depression (top panel), recovery time
411 (middle panel) and survival time (bottom panel).

412

413 **Figure 5.** QTL mapping of respiratory depression in DO mice. **(A)** Genome wide scan for QTL regulating
414 the phenotype of respiratory depression in 300 DO mice. **(B)** Allele effect plot of the LOD 9.2 QTL on
415 chromosome 5 for respiratory depression showing a strong narrow peak with LOD confidence interval of
416 24.98-26.16 MBp. **(C)** A 2MBp interval around the peak locus on chromosome 5 showing the SNPs
417 driving the QTL as well as the genomic features within the interval on chromosome 5.

418

419 **Figure 6.** Protein sequence alignment between WSB/EiJ (WSB) and NOD/ShiLtJ (NOD) mice isoforms
420 of GALNT11. The translated GALTNT11 protein sequence encoded by QTL driving alleles WSB and
421 NOD demonstrate sequence homology except for S545L (*red circle*). Yellow=C (capable of disulfide
422 bonding), Green=A, I, L, M, G, P, V (Hydrophobic) Dark Blue= D, E (Negative Charge) , Dark Green
423 =H, W, Y, F (Aromatic/Hydrophobic) Magenta= R,K (Positive Charge) light blue/purple=T, S, Q, N
424 (Polar)

425

426 **Figure 7.** S545L occurs in the Ricin B lectin domain of GALNT11. **(A)** Multi-species alignment of the
427 Ricin B lectin domain of GALNT11 showing that the S545L mutation occurs in a domain conserved
428 across multiple vertebrates, including humans, mice, rats, *Xenopus*, and zebrafish. **(B)** Protein domain
429 map of human GALNT11 showing the localization of the conserved S545L in the Ricin B lectin domain
430 (*black circle*). The 3D structure rendered showing secondary structure as a cartoon type with coloring as
431 a rainbow from N- to C-terminus.

432

433 **Figure S1. Mapping of the DO survival data using a Cox Proportional-Hazards Model** **(A)** Survival
434 time of male (M, blue) and female (F, red) DO mice as represented by a Cox Proportional-Hazards
435 Model. **(B)** The difference of these log likelihoods was taken and then divided by ln (10) to convert the
436 result to the LOD scale. **(B)** Cox Proportional Hazards (COXPH) QTL mapping model which includes
437 the genotype probabilities. **(D)** Allele effect plot of suggestive chromosome 2 locus.

438 **Table S1.** The 1,885 SNPs that differ between NOD and WSB within the Chromosome 5 QTL interval.

439 **Table S2.** The 287 genes that are known targets for GALNT11 and expressed in the pre-Botzinger

440 complex

441 **Acknowledgements** Funding R01 DA037927, R01 AA018776 and P50 DA039841 to EJC, R01
442 DA048890 to JAB, and the NIDA Drug Supply Program. Special thanks to Jennifer Ryan and the Center
443 for Biometric analysis at JAX for use of the PiezoSleep system and to Stephen Krasinski for extensive
444 edits of the manuscript.

445 **References**

446

447

448 1 Boscarino, J. A. *et al.* Risk factors for drug dependence among out-patients on opioid therapy in
449 a large US health-care system. *Addiction* **105**, 1776-1782, doi:10.1111/j.1360-0443.2010.03052.x
450 (2010).

451 2 Comer, S. D. & Cahill, C. M. Fentanyl: Receptor pharmacology, abuse potential, and implications
452 for treatment. *Neurosci Biobehav Rev* **106**, 49-57, doi:10.1016/j.neubiorev.2018.12.005 (2019).

453 3 Schmid, C. L. *et al.* Bias Factor and Therapeutic Window Correlate to Predict Safer Opioid
454 Analgesics. *Cell* **171**, 1165-1175 e1113, doi:10.1016/j.cell.2017.10.035 (2017).

455 4 Tomassoni, A. J. *et al.* Multiple Fentanyl Overdoses - New Haven, Connecticut, June 23, 2016.
456 *MMWR Morb Mortal Wkly Rep* **66**, 107-111, doi:10.15585/mm6604a4 (2017).

457 5 May, W. J. *et al.* Morphine has latent deleterious effects on the ventilatory responses to a
458 hypoxic-hypercapnic challenge. *Open J Mol Integr Physiol* **3**, 134-145,
459 doi:10.4236/ojmip.2013.33019 (2013).

460 6 Pattinson, K. T. Opioids and the control of respiration. *Br J Anaesth* **100**, 747-758,
461 doi:10.1093/bja/aen094 (2008).

462 7 Frischknecht, H. R., Siegfried, B. & Waser, P. G. Opioids and behavior: genetic aspects.
463 *Experientia* **44**, 473-481 (1988).

464 8 Baran, A., Shuster, L., Eleftheriou, B. E. & Bailey, D. W. Opiate receptors in mice: genetic
465 differences. *Life sciences* **17**, 633-640 (1975).

466 9 Shigeta, Y. *et al.* Association of morphine-induced antinociception with variations in the 5'
467 flanking and 3' untranslated regions of the mu opioid receptor gene in 10 inbred mouse strains.
468 *Pharmacogenetics and genomics* **18**, 927-936, doi:10.1097/FPC.0b013e32830d0b9e (2008).

469 10 Juni, A., Klein, G., Pintar, J. E. & Kest, B. Nociception increases during opioid infusion in opioid
470 receptor triple knock-out mice. *Neuroscience* **147**, 439-444,
471 doi:10.1016/j.neuroscience.2007.04.030 (2007).

472 11 Saito, M. *et al.* Variants of kappa-opioid receptor gene and mRNA in alcohol-preferring and
473 alcohol-avoiding mice. *Alcohol* **29**, 39-49, doi:10.1016/s0741-8329(02)00322-1 (2003).

474 12 Kest, B., Hopkins, E., Palmese, C. A., Adler, M. & Mogil, J. S. Genetic variation in morphine
475 analgesic tolerance: a survey of 11 inbred mouse strains. *Pharmacology, biochemistry, and*
476 *behavior* **73**, 821-828 (2002).

477 13 Wilson, S. G. *et al.* The heritability of antinociception: common pharmacogenetic mediation of
478 five neurochemically distinct analgesics. *The Journal of pharmacology and experimental*
479 *therapeutics* **304**, 547-559, doi:10.1124/jpet.102.041889 (2003).

480 14 Kest, B., Palmese, C. A., Juni, A., Chesler, E. J. & Mogil, J. S. Mapping of a quantitative trait locus
481 for morphine withdrawal severity. *Mammalian genome : official journal of the International*
482 *Mammalian Genome Society* **15**, 610-617, doi:10.1007/s00335-004-2367-3 (2004).

483 15 Smith, S. B. *et al.* Quantitative trait locus and computational mapping identifies Kcnj9 (GIRK3) as
484 a candidate gene affecting analgesia from multiple drug classes. *Pharmacogenetics and*
485 *genomics* **18**, 231-241, doi:10.1097/FPC.0b013e3282f55ab2 (2008).

486 16 Roerig, S. C. & Fujimoto, J. M. Morphine antinociception in different strains of mice: relationship
487 of supraspinal-spinal multiplicative interaction to tolerance. *The Journal of pharmacology and*
488 *experimental therapeutics* **247**, 603-608 (1988).

489 17 Belknap, J. K., Noordewier, B. & Lame, M. Genetic dissociation of multiple morphine effects
490 among C57BL/6J, DBA/2J and C3H/HeJ inbred mouse strains. *Physiology & behavior* **46**, 69-74
491 (1989).

492 18 Philip, V. M. *et al.* High-throughput behavioral phenotyping in the expanded panel of BXD
493 recombinant inbred strains. *Genes Brain Behav* **9**, 129-159, doi:GBB540 [pii]

494 10.1111/j.1601-183X.2009.00540.x (2010).

495 19 Bohn, L. M., Gainetdinov, R. R., Lin, F. T., Lefkowitz, R. J. & Caron, M. G. Mu-opioid receptor
496 desensitization by beta-arrestin-2 determines morphine tolerance but not dependence. *Nature*
497 **408**, 720-723, doi:10.1038/35047086 (2000).

498 20 Belknap, J. K. & Crabbe, J. C. Chromosome mapping of gene loci affecting morphine and
499 amphetamine responses in BXD recombinant inbred mice. *Annals of the New York Academy of*
500 *Sciences* **654**, 311-323 (1992).

501 21 Fechtner, L., El Ali, M., Sattar, A., Moore, M. & Strohl, K. P. Fentanyl effects on breath generation
502 in C57BL/6J and A/J mouse strains. *Respiratory physiology & neurobiology* **215**, 20-29,
503 doi:10.1016/j.resp.2015.04.011 (2015).

504 22 Muraki, T. & Kato, R. Strain difference in the effects of morphine on the rectal temperature and
505 respiratory rate in male mice. *Psychopharmacology* **89**, 60-64 (1986).

506 23 Yoburn, B. C., Kreuscher, S. P., Inturrisi, C. E. & Sierra, V. Opioid receptor upregulation and
507 supersensitivity in mice: effect of morphine sensitivity. *Pharmacology, biochemistry, and*
508 *behavior* **32**, 727-731 (1989).

509 24 Moskowitz, A. S., Terman, G. W., Carter, K. R., Morgan, M. J. & Liebeskind, J. C. Analgesic,
510 locomotor and lethal effects of morphine in the mouse: strain comparisons. *Brain research* **361**,
511 46-51 (1985).

512 25 Nasser, S. A. & Afify, E. A. Sex differences in pain and opioid mediated antinociception:
513 Modulatory role of gonadal hormones. *Life sciences* **237**, 116926, doi:10.1016/j.lfs.2019.116926
514 (2019).

515 26 Donohue, K. D., Medonza, D. C., Crane, E. R. & O'Hara, B. F. Assessment of a non-invasive high-
516 throughput classifier for behaviours associated with sleep and wake in mice. *Biomedical*
517 *engineering online* **7**, 14, doi:10.1186/1475-925X-7-14 (2008).

518 27 Philip, V. M. *et al.* Genetic analysis in the Collaborative Cross breeding population. *Genome*
519 *research* **21**, 1223-1238, doi:10.1101/gr.113886.110 (2011).

520 28 Bubier, J. A. *et al.* A Microbe Associated with Sleep Revealed by a Novel Systems Genetic
521 Analysis of the Microbiome in Collaborative Cross Mice. *Genetics* **214**, 719-733,
522 doi:10.1534/genetics.119.303013 (2020).

523 29 Hou, T. *et al.* Active Time-Restricted Feeding Improved Sleep-Wake Cycle in db/db Mice. *Front*
524 *Neurosci* **13**, 969, doi:10.3389/fnins.2019.00969 (2019).

525 30 Broman, K. R/qtl2 : QTL analysis for high-dimensional data and complex crosses,
526 <<https://kbroman.org/qtl2/>> (

527 31 Durrant, C. *et al.* Collaborative Cross mice and their power to map host susceptibility to
528 Aspergillus fumigatus infection. *Genome research* **21**, 1239-1248, doi:10.1101/gr.118786.110
529 (2011).

530 32 Hayes, J. A. *et al.* Transcriptome of neonatal preBotzinger complex neurones in Dbx1 reporter
531 mice. *Scientific reports* **7**, 8669, doi:10.1038/s41598-017-09418-4 (2017).

532 33 Hintze, J. *et al.* Probing the contribution of individual polypeptide GalNAc-transferase isoforms
533 to the O-glycoproteome by inducible expression in isogenic cell lines. *The Journal of biological
534 chemistry* **293**, 19064-19077, doi:10.1074/jbc.RA118.004516 (2018).

535 34 Baker, E., Bubier, J. A., Reynolds, T., Langston, M. A. & Chesler, E. J. GeneWeaver: data driven
536 alignment of cross-species genomics in biology and disease. *Nucleic acids research* **44**, D555-
537 559, doi:10.1093/nar/gkv1329 (2016).

538 35 Juul, S. E., Beyer, R. P., Bammler, T. K., Farin, F. M. & Gleason, C. A. Effects of neonatal stress and
539 morphine on murine hippocampal gene expression. *Pediatr Res* **69**, 285-292,
540 doi:10.1203/PDR.0b013e31820bd165 (2011).

541 36 Anghel, A. *et al.* Gene expression profiling following short-term and long-term morphine
542 exposure in mice uncovers genes involved in food intake. *Neuroscience* **167**, 554-566,
543 doi:10.1016/j.neuroscience.2010.01.043 (2010).

544 37 Le Merrer, J. *et al.* Protracted abstinence from distinct drugs of abuse shows regulation of a
545 common gene network. *Addict Biol* **17**, 1-12, doi:10.1111/j.1369-1600.2011.00365.x (2012).

546 38 Davis, A. P. *et al.* The Comparative Toxicogenomics Database: update 2019. *Nucleic acids
547 research* **47**, D948-D954, doi:10.1093/nar/gky868 (2019).

548 39 Shibusaki, M., Katsura, M., Kurokawa, K., Torigoe, F. & Ohkuma, S. Regional differences of L-type
549 high voltage-gated calcium channel subunit expression in the mouse brain after chronic
550 morphine treatment. *J Pharmacol Sci* **105**, 177-183, doi:10.1254/jphs.fp0070885 (2007).

551 40 Brick, L. A., Micalizzi, L., Knopik, V. S. & Palmer, R. H. C. Characterization of DSM-IV Opioid
552 Dependence Among Individuals of European Ancestry. *J Stud Alcohol Drugs* **80**, 319-330 (2019).

553 41 Cheng, Z. *et al.* Genome-wide Association Study Identifies a Regulatory Variant of RGMA
554 Associated With Opioid Dependence in European Americans. *Biol Psychiatry* **84**, 762-770,
555 doi:10.1016/j.biopsych.2017.12.016 (2018).

556 42 Smith, A. H. *et al.* Genome-wide association study of therapeutic opioid dosing identifies a novel
557 locus upstream of OPRM1. *Mol Psychiatry* **22**, 346-352, doi:10.1038/mp.2016.257 (2017).

558 43 Gelernter, J. *et al.* Genome-wide association study of opioid dependence: multiple associations
559 mapped to calcium and potassium pathways. *Biol Psychiatry* **76**, 66-74,
560 doi:10.1016/j.biopsych.2013.08.034 (2014).

561 44 Nelson, E. C. *et al.* Evidence of CNIH3 involvement in opioid dependence. *Mol Psychiatry* **21**,
562 608-614, doi:10.1038/mp.2015.102 (2016).

563 45 Nishizawa, D. *et al.* Genome-wide association study identifies a potent locus associated with
564 human opioid sensitivity. *Mol Psychiatry* **19**, 55-62, doi:10.1038/mp.2012.164 (2014).

565 46 Yang, B. Z., Han, S., Kranzler, H. R., Palmer, A. A. & Gelernter, J. Sex-specific linkage scans in
566 opioid dependence. *Am J Med Genet B Neuropsychiatr Genet* **174**, 261-268,
567 doi:10.1002/ajmg.b.32507 (2017).

568 47 Montalvo-Ortiz, J. L., Cheng, Z., Kranzler, H. R., Zhang, H. & Gelernter, J. Genomewide Study of
569 Epigenetic Biomarkers of Opioid Dependence in European-American Women. *Scientific reports*
570 **9**, 4660, doi:10.1038/s41598-019-41110-7 (2019).

571 48 Li, D. *et al.* Genome-wide association study of copy number variations (CNVs) with opioid
572 dependence. *Neuropsychopharmacology* **40**, 1016-1026, doi:10.1038/npp.2014.290 (2015).

573 49 Polimanti, R. *et al.* Leveraging genome-wide data to investigate differences between opioid use
574 vs. opioid dependence in 41,176 individuals from the Psychiatric Genomics Consortium. *Mol*
575 *Psychiatry*, doi:10.1038/s41380-020-0677-9 (2020).

576 50 Cheng, Z. *et al.* Genome-wide scan identifies opioid overdose risk locus close to MCOLN1. *Addict*
577 *Biol*, e12811, doi:10.1111/adb.12811 (2019).

578 51 Delprato, A. *et al.* QTL and systems genetics analysis of mouse grooming and behavioral
579 responses to novelty in an open field. *Genes Brain Behav* **16**, 790-799, doi:10.1111/gbb.12392
580 (2017).

581 52 Recla, J. M. *et al.* Genetic mapping in Diversity Outbred mice identifies a Trpa1 variant
582 influencing late-phase formalin response. *Pain* **160**, 1740-1753,
583 doi:10.1097/j.pain.0000000000001571 (2019).

584 53 Recla, J. M. *et al.* Precise genetic mapping and integrative bioinformatics in Diversity Outbred
585 mice reveals Hydin as a novel pain gene. *Mammalian genome : official journal of the*
586 *International Mammalian Genome Society* **25**, 211-222, doi:10.1007/s00335-014-9508-0 (2014).

587 54 Petaja-Repo, U. E., Hogue, M., Laperriere, A., Walker, P. & Bouvier, M. Export from the
588 endoplasmic reticulum represents the limiting step in the maturation and cell surface expression
589 of the human delta opioid receptor. *The Journal of biological chemistry* **275**, 13727-13736
590 (2000).

591 55 Egletton, R. D. *et al.* Improved blood-brain barrier penetration and enhanced analgesia of an
592 opioid peptide by glycosylation. *The Journal of pharmacology and experimental therapeutics*
593 **299**, 967-972 (2001).

594 56 Flores, A. E. *et al.* Pattern recognition of sleep in rodents using piezoelectric signals generated by
595 gross body movements. *IEEE transactions on bio-medical engineering* **54**, 225-233,
596 doi:10.1109/TBME.2006.886938 (2007).

597 57 Mohrland, J. S. & Craigmill, A. L. Possible mechanism for the enhanced lethality of morphine in
598 aggregated mice. *Pharmacology, biochemistry, and behavior* **13**, 475-477 (1980).

599 58 Campos, A. E., Lujan, M., Lopez, E., Figueroa-Hernandez, J. L. & Rodriguez, R. Circadian variation
600 in the lethal effect of morphine in the mouse. *Proceedings of the Western Pharmacology Society*
601 **26**, 101-103 (1983).

602 59 (2016).

603 60 Ritz, C., Baty, F., Streibig, J. C. & Gerhard, D. Dose-Response Analysis Using R. *PLoS One* **10**,
604 e0146021, doi:10.1371/journal.pone.0146021 (2015).

605 61 Bates, D. M. & Watts, D. G. *Nonlinear regression analysis and its applications*. (Wiley, 1988).

606 62 Chick, J. M. *et al.* Defining the consequences of genetic variation on a proteome-wide scale.
607 *Nature* **534**, 500-505, doi:10.1038/nature18270 (2016).

608 63 Broman, K. W. *et al.* R/qtl2: Software for Mapping Quantitative Trait Loci with High-Dimensional
609 Data and Multiparent Populations. *Genetics* **211**, 495-502, doi:10.1534/genetics.118.301595
610 (2019).

611 64 Churchill, G. A. & Doerge, R. W. Empirical threshold values for quantitative trait mapping.
612 *Genetics* **138**, 963-971 (1994).

613 65 Sen, S. & Churchill, G. A. A statistical framework for quantitative trait mapping. *Genetics* **159**,
614 371-387 (2001).

615 66 Yalcin, B. *et al.* Sequence-based characterization of structural variation in the mouse genome.
616 *Nature* **477**, 326-329, doi:10.1038/nature10432 (2011).

617 67 Bult, C. J. *et al.* Mouse Genome Database (MGD) 2019. *Nucleic acids research* **47**, D801-D806,
618 doi:10.1093/nar/gky1056 (2019).

619 68 van Lunteren, E., Moyer, M. & Leahy, P. Gene expression profiling of diaphragm muscle in
620 alpha2-laminin (merosin)-deficient dy/dy dystrophic mice. *Physiol Genomics* **25**, 85-95,
621 doi:10.1152/physiolgenomics.00226.2005 (2006).

622 69 Steed, A. L. *et al.* The microbial metabolite desaminotyrosine protects from influenza through
623 type I interferon. *Science* **357**, 498-502, doi:10.1126/science.aam5336 (2017).

624 70 Sievers, F. *et al.* Fast, scalable generation of high-quality protein multiple sequence alignments
625 using Clustal Omega. *Mol Syst Biol* **7**, 539, doi:10.1038/msb.2011.75 (2011).

626 71 Soding, J. Protein homology detection by HMM-HMM comparison. *Bioinformatics* **21**, 951-960,
627 doi:10.1093/bioinformatics/bti125 (2005).

628 72 Fritz, T. A., Hurley, J. H., Trinh, L. B., Shiloach, J. & Tabak, L. A. The beginnings of mucin
629 biosynthesis: the crystal structure of UDP-GalNAc:polypeptide alpha-N-
630 acetylgalactosaminyltransferase-T1. *Proc Natl Acad Sci U S A* **101**, 15307-15312,
631 doi:10.1073/pnas.0405657101 (2004).

632 73 team, J. d. *Jmol: an open-source Java viewer for chemical structures in 3D.*,
633 <<http://www.jmol.org/>> (2001).

634

Figure 1

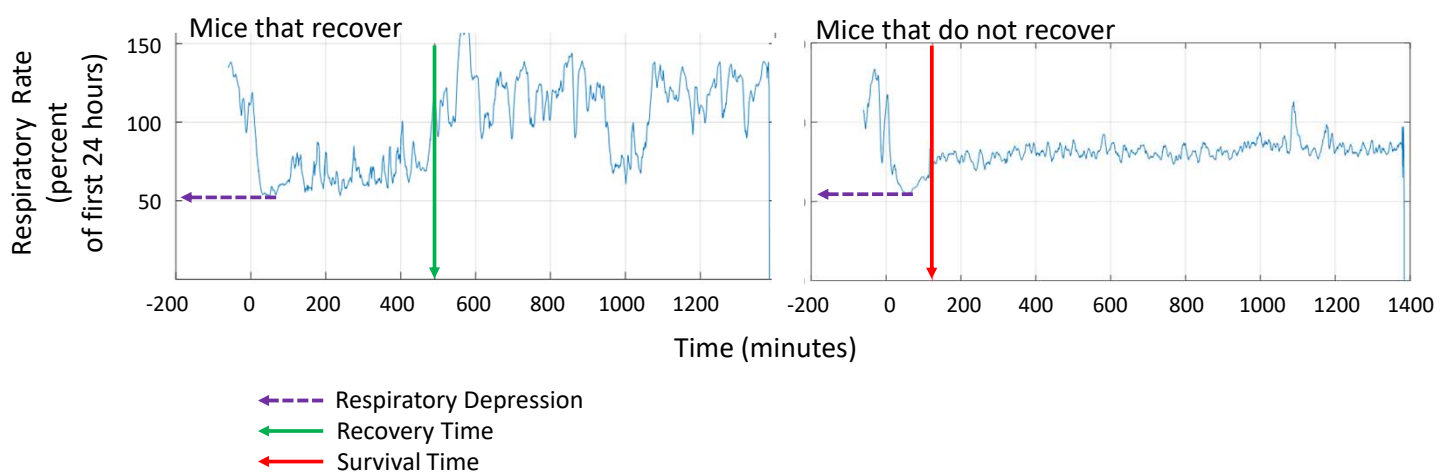


Figure 2

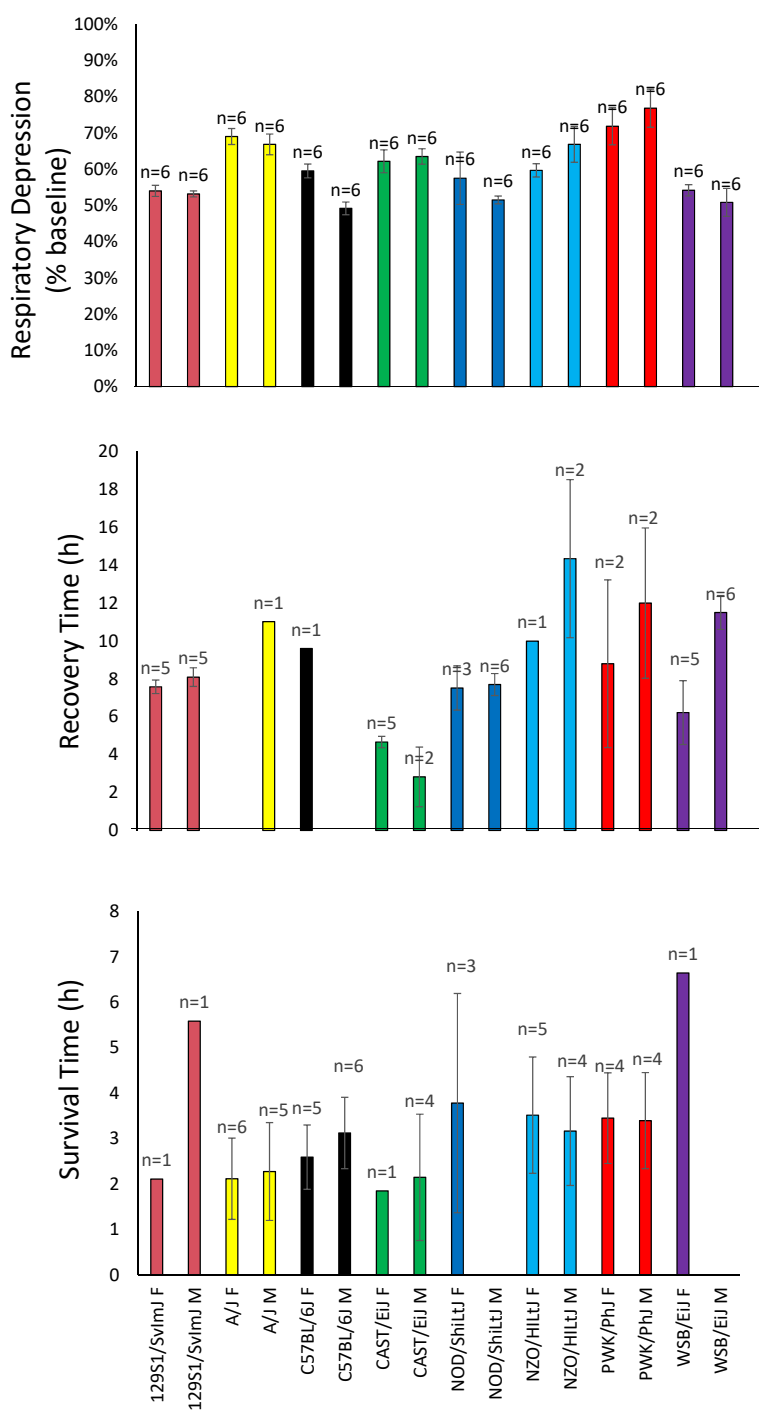
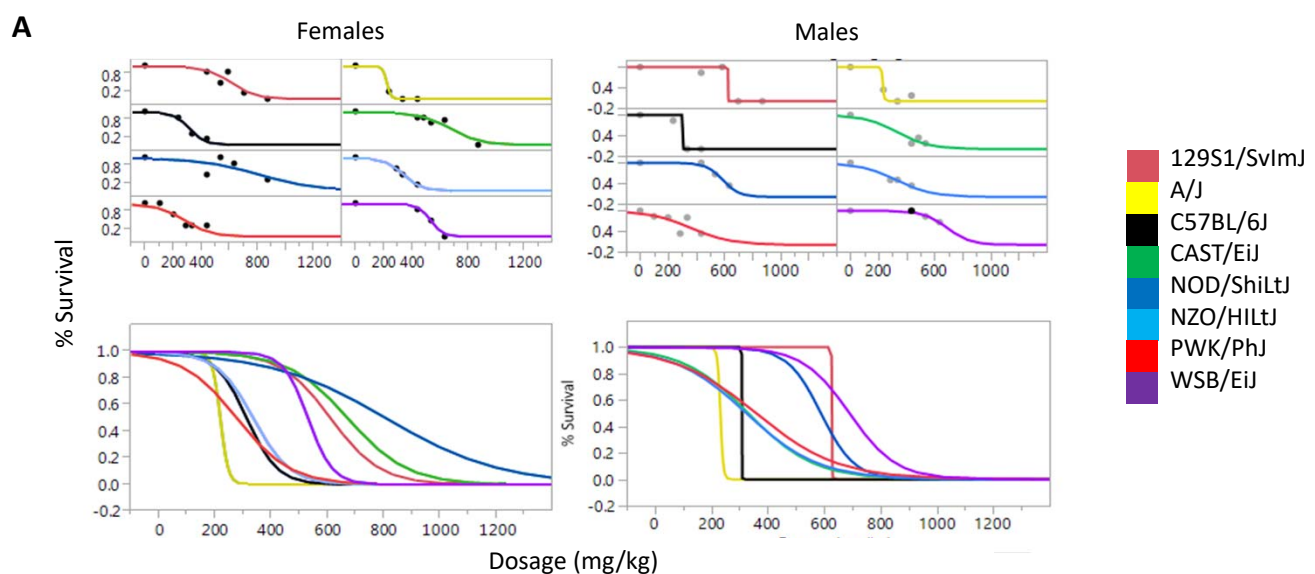


Figure 3



B

Strain and Sex	LD ₅₀ Morphine (mg/kg)
129S1/SvImJ F	631.3
129S1/SvImJ M	664.2
A/J F	212.2
A/J M	225.2
C57BL/6J F	311.6
C57BL/6J M	254.3
CAST/EiJ F	882.2
CAST/EiJ M	429.9
NOD/ShiLtJ F	811.0
NOD/ShiLtJ M	588.8
NZO/HILtJ F	333.9
NZO/HILtJ M	324.4
PWK/PhJ F	261.0
PWK/PhJ M	359.1
WSB/EiJ F	526.4
WSB/EiJ M	695.6

Figure 4

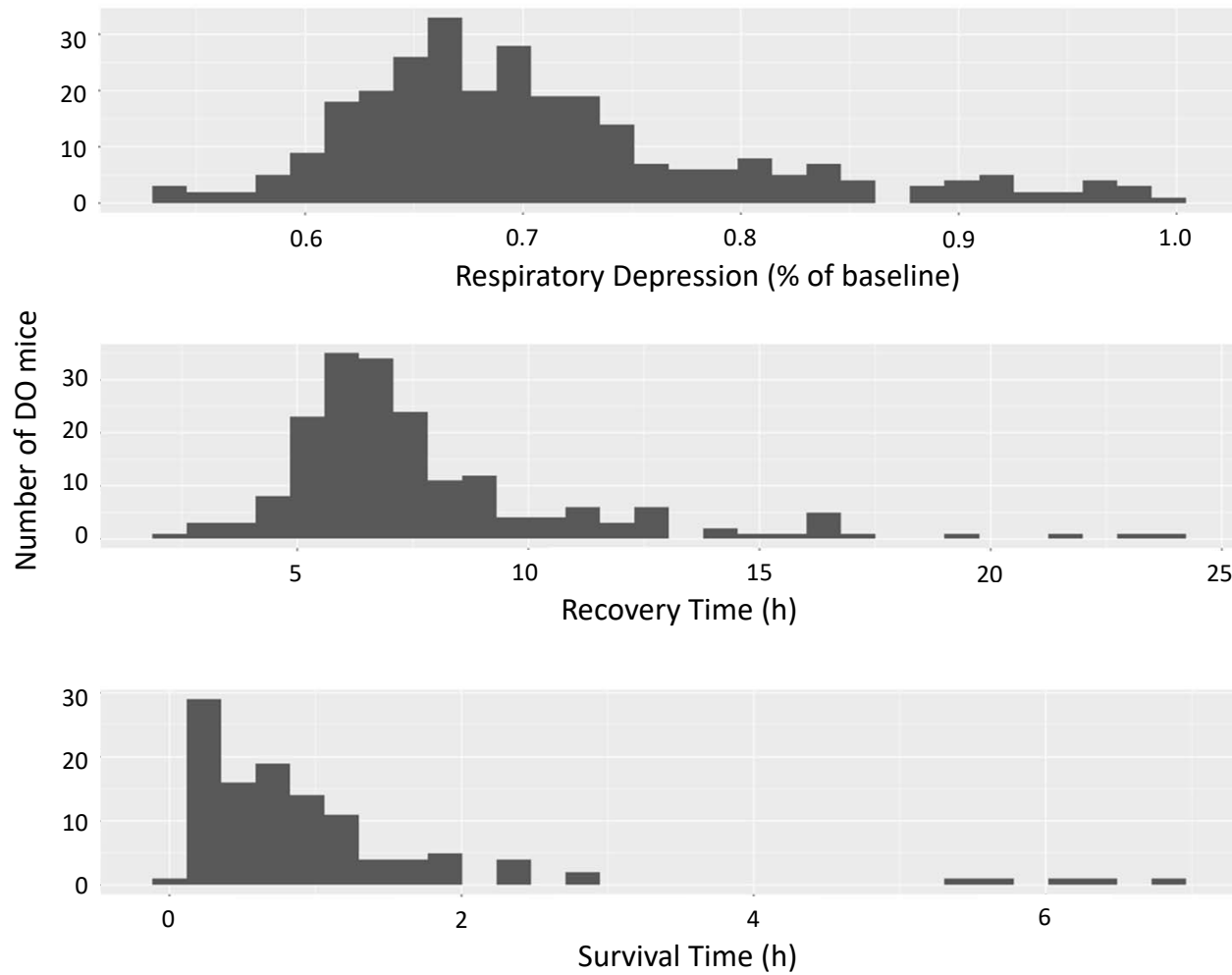
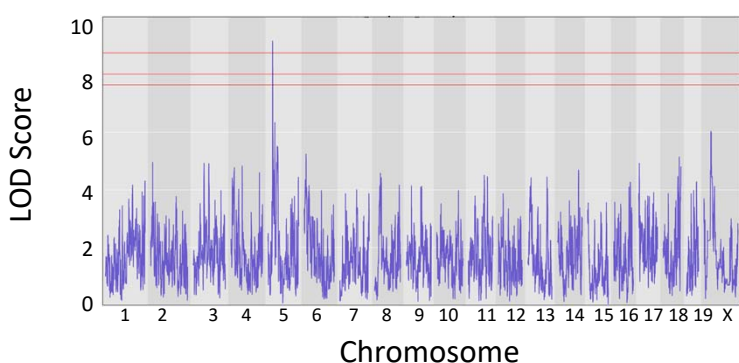
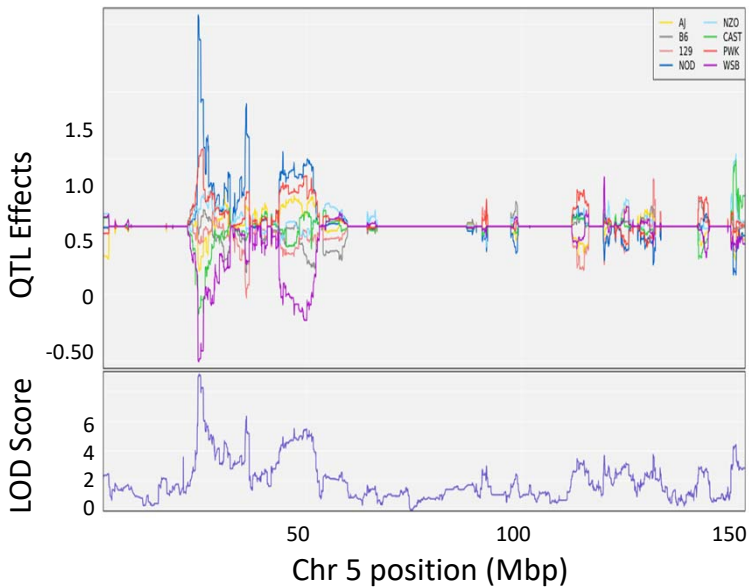


Figure 5

A



B



C

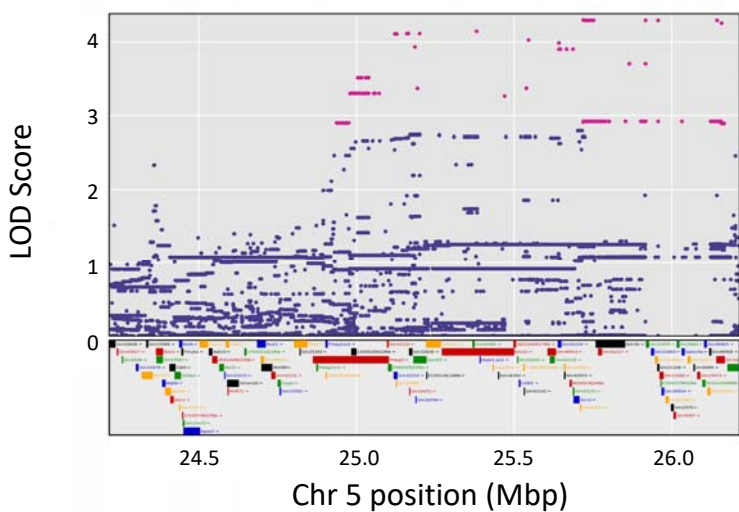


Figure 6

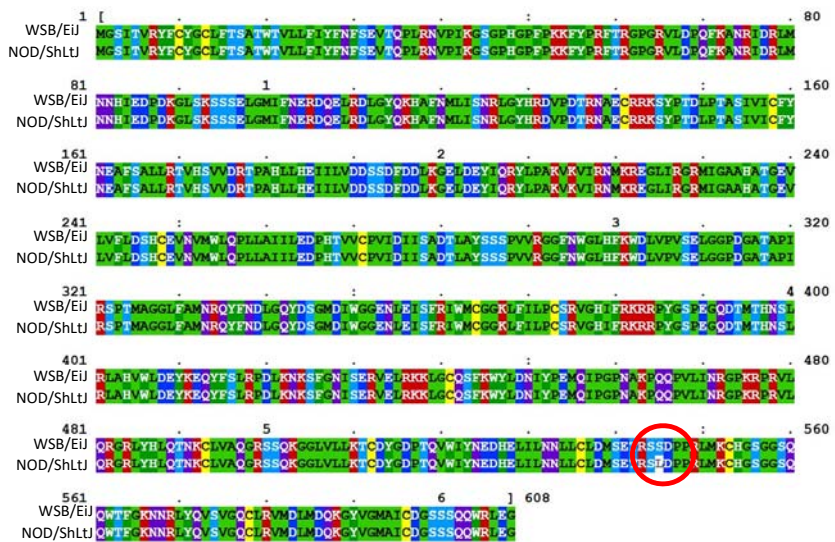


Figure 7

A

Ricin B-type lectin domain

B

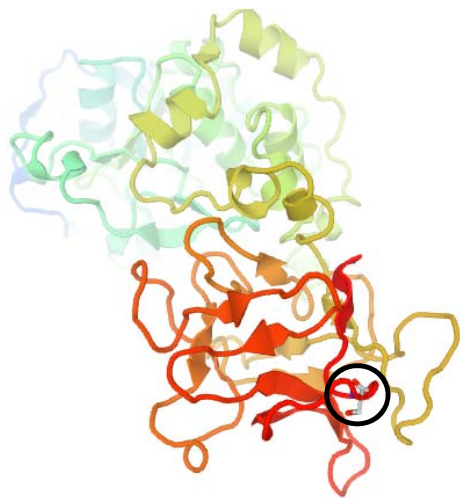
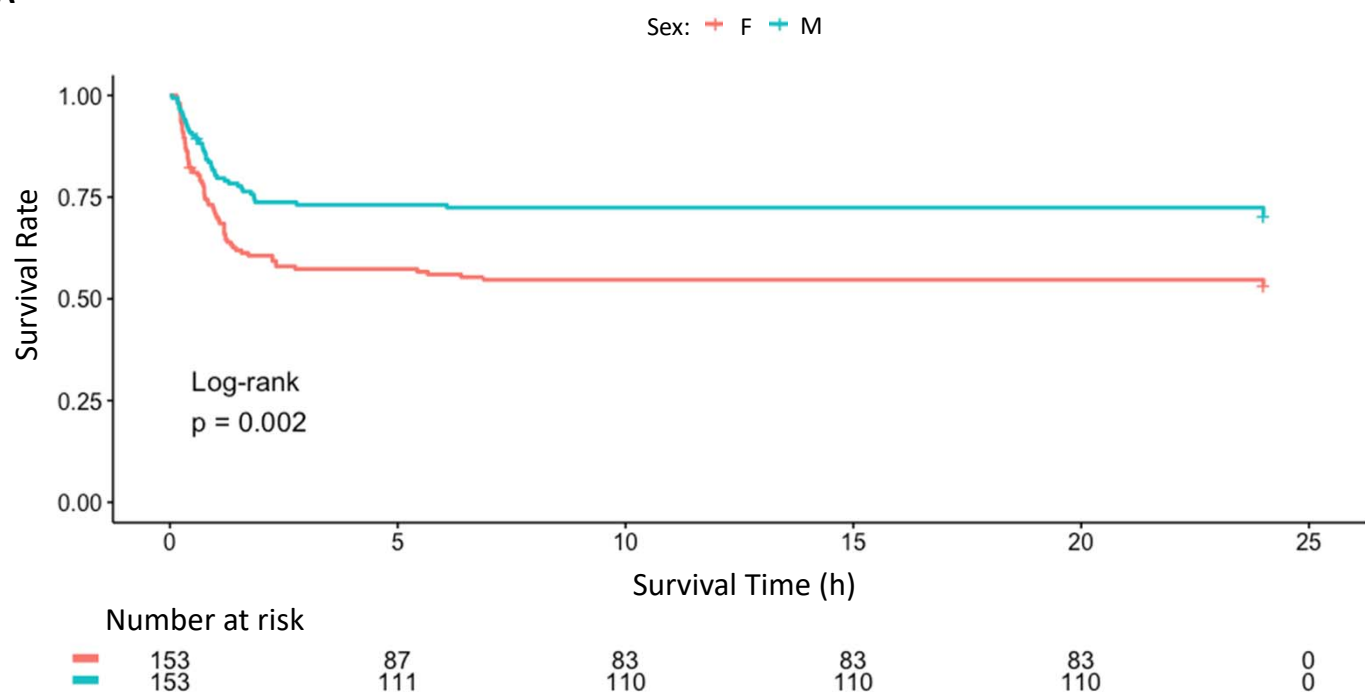
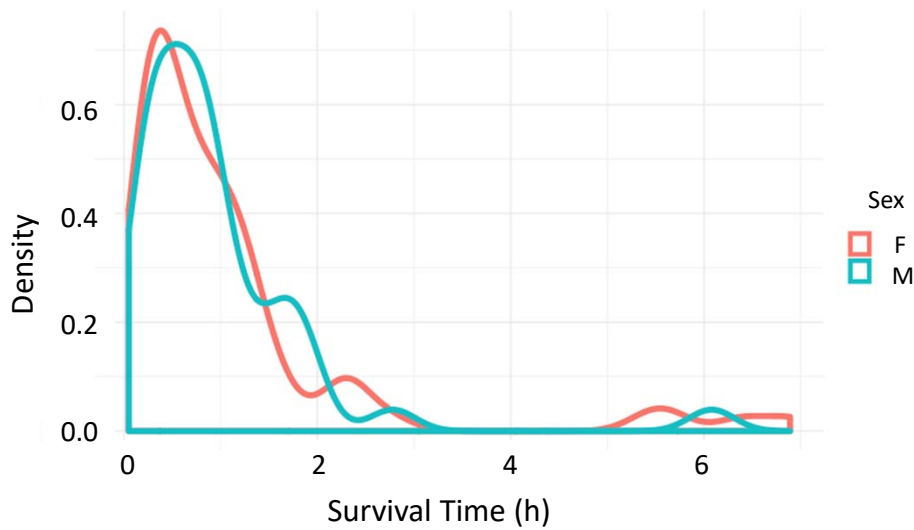


Figure S1

A



B



Supplemental Figure 1 C and D

